Narrow-band tunable extreme-ultraviolet laser source for lifetime measurements and precision spectroscopy

W. Ubachs, K. S. E. Eikema, and W. Hogervorst

Laser Centre, Department of Physics and Astronomy, Vrije Universiteit De Boelelaan 1081, 1081 HV Amsterdam, the Netherlands

P. C. Cacciani

Laboratoire Aimé Cotton, Campus d'Université Paris-Sud, Orsay Cedex, France

Received November 6, 1996; revised manuscript received March 24, 1997

A narrow-band, extreme-ultraviolet laser source is developed that has continuous tunability in the range 96–97.5 nm and a bandwidth below 250 MHz. The versatility of the radiation source is demonstrated in two applications. Accurate values for lifetimes of highly excited molecular quantum states are determined from line-broadening measurements in three electronic states of CO: $W^1\Pi$, $v = 0$ state (Π_f components, $J = 1–3$), $\tau = 130 \pm 10$ ps; $L^1\Pi$, $v = 0$ state (Π_f components, $J = 1–6$), $\tau = 1.0 \pm 0.3$ ns; and $K^1\Sigma^+$, $v = 0$ state ($J = 0–3$), $\tau = 54 \pm 5$ ps. The application of the source in metrology in the extreme-ultraviolet domain is demonstrated by the highly accurate, absolute calibration of narrow resonances in CO. These molecular lines can be used for future reference standards at these short wavelengths. From accurately determined minute frequency shifts near the accidentally predissociated $J_f = 7$ level of the $L^1\Pi$, $v = 0$ state the perturber state is characterized as a yet unidentified Rydberg state with an origin at 103 266.92 cm^{-1}. It is demonstrated that molecular spectroscopy in the extreme-ultraviolet domain at megahertz precision is possible. [S0740-3224(97)00810-2]

1. INTRODUCTION

Radiation in the extreme-ultraviolet (XUV) wavelength part of the electromagnetic spectrum, defined here as the range 50–100 nm, is routinely produced with classical discharges of noble gases, synchrotrons, and laser-induced plasmas. These sources have in common that they are intrinsically broadband. In spectroscopic applications, where resolution is of relevance, these instruments are combined with monochromators, which then are the bandwidth-limiting factors. Through harmonic generation of the output of powerful pulsed-dye lasers, tunable radiation in the XUV domain can be generated with bandwidths determined by the spectral purity of the incident laser beams. In the case when Fourier-transform-limited pulses of nanosecond duration are used as fundamentals, extremely narrow bandwidths at wavelengths in the XUV domain can be generated by harmonic conversion. In this paper we report on the application of a narrow-band source of XUV radiation, tunable in the range 96–97.5 nm. The high resolving power (250 MHz) in the frequency domain is used to extract information on lifetimes of excited states in molecules by means of line-broadening measurements. In the available wavelength range three electronic states of CO could be accessed: $W^1\Pi$, $v = 0$; $L^1\Pi$, $v = 0$; and $K^1\Sigma^+$, $v = 0$. For both $^1\Pi$ states the lifetimes of the Π_e components have already been investigated in detail by XUV laser excitation.[1] The improved resolution by a factor of 40 now permits a determination of the lifetimes of the longer-lived Π_f components. Lifetimes of these excited states in CO have been determined in the two-color laser spectroscopic experiment by Drabbels *et al.*[2]

An important characteristic of an XUV laser source based on harmonic generation is the possibility for on-line frequency calibration against a reference standard at the fundamental wavelength. For this purpose linear absorption of the pulsed output of the dye lasers in molecular iodine is usually employed[1,3,4] or, in the case of fundamental wavelengths in the blue, linear absorption in molecular tellurium.[5] The accuracy of the I_2 atlas,[6] regularly used for wavelength calibration of pulsed lasers, is limited because of Doppler broadening and asymmetry of the line profiles. Nonlinear saturation spectroscopy of I_2 with the application of cw dye lasers is known to set a more accurate standard.[7–9] Recently we have demonstrated that the latter technique can be combined with pulsed-dye amplification and harmonic generation to set an accurate wavelength standard at 58.4 nm.[10,11] Here the combination of techniques is demonstrated for highly precise XUV spectroscopy of excited states of molecules. For many of the essential experimental details not outlined in the present paper, we refer the reader to Ref. 11.

2. EXPERIMENTAL

The XUV-laser setup and its use for spectroscopic investigations as well as lifetime measurements on CO has been described by Eikema *et al.*[1] However, the present

0740-3224/97/102469-08$10.00

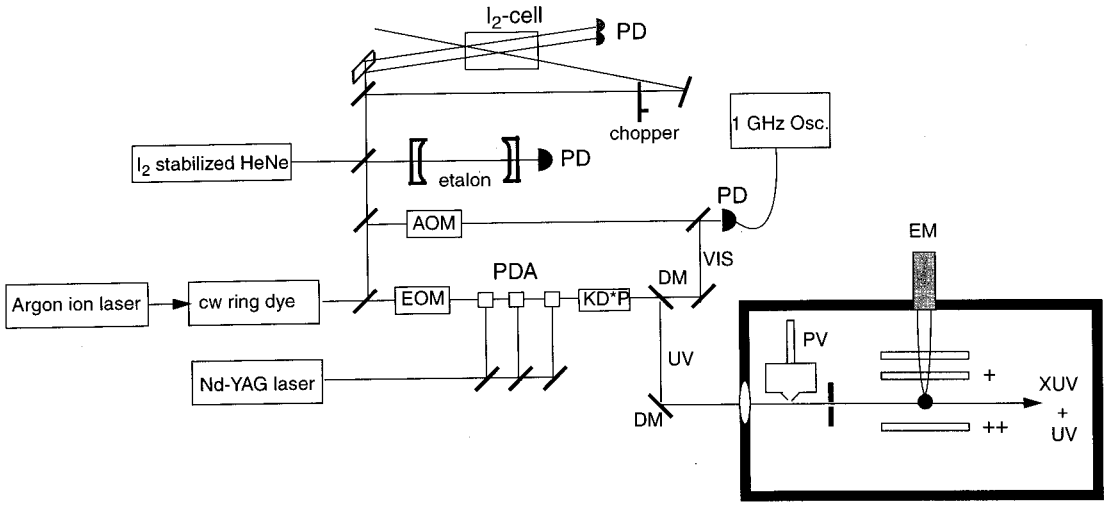

Fig. 1. Schematic of the experimental setup. Overlapping XUV and UV beams perpendicularly intersect a pulsed beam of CO. Ions produced in the interaction zone are accelerated by a pulsed electric field (delayed after the laser pulse) and detected on an electron multiplier (EM). The part within the rectangle in the lower right is in vacuum. The acousto-optic modulator (AOM) shifts the carrier frequency by 250 MHz for analysis of the chirp (see text); the electro-optic modulator (EOM) induces phase changes in the seed beam to compensate for chirp effects. The upper part shows the setup for I_2 saturation spectroscopy. DM, dichroic mirrors; PV, pulsed valve; KD*P, frequency doubling crystal; PD, photodiodes.

setup, displayed schematically in Fig. 1, contains as an important improvement the replacement of the commercial pulsed-dye laser by a home-built, three-stage, pulsed-dye amplifier (PDA) delivering laser pulses of up to 200 mJ/pulse in 6-ns durations. This PDA is pumped by the green output of a Nd:YAG laser, and it pulse amplifies the output of a narrow-band ($\approx$1 MHz) Ar-ion pumped cw ring dye laser. Although the design of the PDA is somewhat different, the main characteristics are similar to the setup used by Cromwell *et al.*[12] The laser system was operated with Rhodamine 6G dye in the cw ring dye laser and Rhodamine B or a mixture of Rhodamines B and 6G in the PDA, which allowed tunability in the range 575–585 nm. After frequency doubling the pulsed output of the PDA in a KD*P crystal, up to 90 mJ/pulse can be generated in the UV, although in the present experiment, UV intensities were limited to 15–30 mJ/pulse. Subsequent frequency tripling in a pulsed-gas jet then yields tunable radiation in the range 96–97.5 nm. The instrumental width of the XUV source was determined by measuring the transition of the ^{84}Kr isotope at 104 887 cm^{-1} in a crossed-molecular-beam–laser-beam configuration and applying 1 XUV+1 UV photoionization detection. Care was taken to produce a well-collimated atomic beam by means of a skimmer, so that residual Doppler effects are minimal. This bandwidth calibration resulted in a value of 250 $\pm$ 30 MHz for the instrumental width. This width is determined by the simultaneous registration of frequency markers from a stabilized etalon [free spectral range (FSR) of 148.9560 (5) MHz] with the output of the cw ring dye laser. It turned out that the Kr resonance was easily saturated by the XUV power, giving rise to additional broadening. For CO no such broadening was observed, which may be explained by the fact that the oscillator strength for each individual rotational line is much smaller owing to the rovibrational distribution of oscillator strength. The instrument function was determined from a low-intensity measurement. The particular $5p^6-6s'$ resonance in Kr was selected because the excited-state lifetime is sufficiently long (100 ns)[3] that it does not contribute to the observed linewidth. The resulting 250 MHz is due predominantly to the bandwidth of the XUV-radiation source, while a minor contribution from residual Doppler effects may still be present. It is conceivable that the bandwidth is intensity dependent. However, from detailed studies of chirp effects in the PDA,[11] it follows that the chirp (the main source of bandwidth beyond the Fourier limit) does not increase at high output powers of the PDA.

Excited states of CO were probed in the same configuration, also by 1 XUV + 1 UV photoionization. Natural linewidths of the excited states of CO corresponding to the excited-state lifetimes were obtained by deconvolving the instrumental width from the measured linewidths. The linewidths derive again from relative frequency measurements by use of the etalon. In addition to line-broadening measurements, attention was given to improvement of the spectroscopy, particularly of the extremely narrow, singly resolved rotational Q-branch lines of the $L-X$ (0, 0) band. Absolute frequencies could be determined from simultaneous on-line registration of the I_2-saturation spectrum with the output of the cw ring dye laser. Frequencies of the CO lines are then determined by measuring distances between resonances on the XUV scale and the I_2-saturation peaks at the fundamental in terms of etalon fringes and then multiplying the result by a factor of six for harmonic conversion. The saturation signal is monitored by measuring the differential absorption of two probe beams traversing a sealed-off I_2 cell with room-temperature vapor pressure (see Fig. 1).

One of the probe beams partially overlaps a modulated intense beam, saturating the I_2-transitions.

An essential problem related to the frequency comparison of pulsed and cw lasers is that of frequency chirp: the time-dependent variation of the frequency during the laser pulse. Such a chirp effect gives rise to a net shift between the stable and narrow-band frequency of the cw beam and the center frequency of the pulsed output, which is of course broadened owing to its pulse structure. The chirp in our PDA system was measured by registration of the beat note between its pulsed output and the cw input, which for this purpose was shifted over 250 MHz with an acousto-optic modulator (see Fig. 1). Chirp occurs as changes in the phase evolution, which is monitored on a fast (1 GHz, 5 Gs/s) digital oscilloscope; the frequency chirp can be reconstructed from the observed phase patterns. This chirp effect can be counteracted by imposing fast phase changes on the seed beam entering the PDA system by an electro-optic modulator. This method of generating chirp-free pulses is applied here for the accurate and absolute calibration of CO lines. For more details on this method, see Ref. 11.

3. RESULTS

A. Lifetime Measurements

Three excited states of CO that can be excited within the scan range of our narrow-band XUV source were investigated: the $4p\sigma\, X^+(0)$ state of $^1\Sigma^+$ symmetry (referred to as the $K^1\Sigma^+$ state), the $3s\sigma A^+(0)$ state of $^1\Pi$ symmetry (referred to as the $W^1\Pi$ state), and the $4p\pi\, X^+(0)$ state of $^1\Pi$ symmetry (referred to as the $L^1\Pi$ state). Recordings of singly resolved rotational lines are presented in Fig. 2 for the $R(0)$ line of the $K–X$ $(0, 0)$ band, in Fig. 3 for the $Q(1)$ and $Q(2)$ lines of the $W–X$ $(0, 0)$ band, and in Fig. 4 for the Q-bandhead region of the $L–X$ $(0, 0)$ band, which is resolved for the first time. In the figures' reference spectra, either etalon-marker spectra or a saturated Doppler-free I_2-absorption spectrum are shown as well. For all recordings the etalon spectrum was used to determine the linewidth. As an example, the data of Fig. 2 are fitted to a Voigt profile; the fitted profile is close to a Lorentzian and reproduces the observed line shape quite well. In this way all lines were fitted to a Voigt profile to determine the linewidths $\delta\nu_{\rm obs}$. Values for $\delta\nu_{\rm obs}$ are given in Table 1 for all excited states investigated. Particularly for the low J levels of the $L^1\Pi_f$ state, multiple linewidths were recorded to derive accurate values for $\delta\nu_{\rm obs}$. Since the Doppler contribution to the linewidth was minimized under conditions of a collimated, supersonic, molecular beam expansion, it had a low rotational temperature, and only the low J values could be investigated. The Q branch of the strong $L–X$ band could be followed up to $Q(12)$. As in the observation of Sekine *et al.*,[13] the $Q(7)$ line is completely missing because of an accidental predissociation, as is evident from Fig. 4. In a 1 XUV + 1 UV photoionization experiment the vanishing of a line is an indication of a strong accidental perturbation because the signal intensity strongly depends upon the excited-state lifetime.[1]

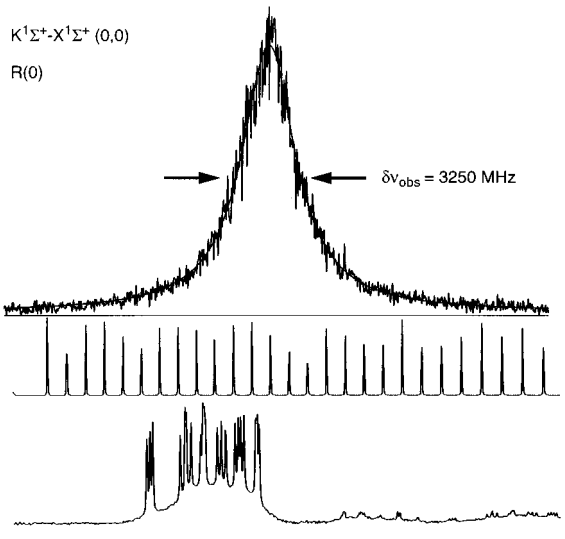

Fig. 2. Spectrum of the $R(0)$ transition of the $K^1\Sigma^+–X^1\Sigma^+(0, 0)$ band of CO recorded by 1XUV + 1UV photoionization at λ = 97.03 nm. Etalon markers (in the middle panel) and an I_2 saturation spectrum (lower panel) are on-line recorded with the output of the cw ring dye laser.

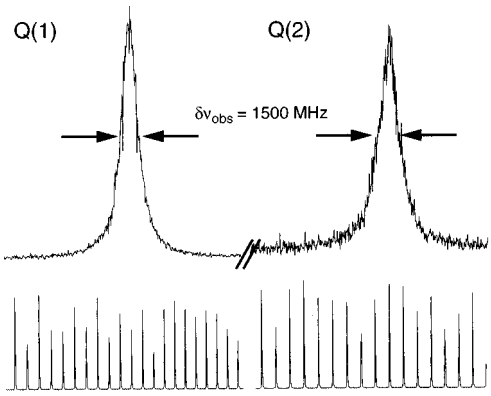

Fig. 3. Spectrum of separately recorded $Q(1)$ and $Q(2)$ lines of the $W^1\Pi–X^1\Sigma^+(0, 0)$ band of CO recorded by 1XUV + 1UV photoionization at λ = 97.27 nm. Also shown are transmission fringes of a stabilized etalon used for the determination of the linewidths.

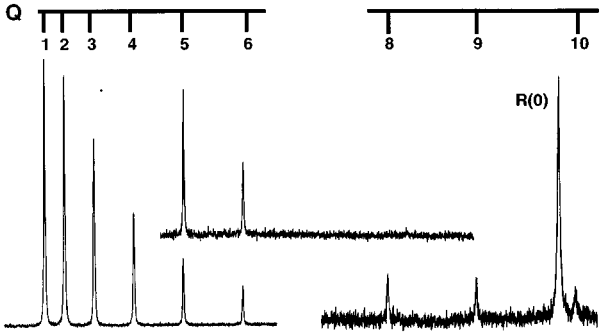

Fig. 4. Excitation spectrum of the $L^1\Pi–X^1\Sigma^+(0, 0)$ band of CO in the bandhead region of the Q branch by 1XUV + 1UV photoionization at λ = 96.83 nm, recorded in three separate overlapping scans. Note that the $Q(7)$ line is missing.

Table 1. Observed Linewidths $\delta\nu_{obs}$, Derived Natural Widths Γ, and Calculated Natural Lifetimes τ for Various States in CO

State		$\delta\nu_{obs}$ (MHz)	Γ (MHz)	τ (ps)
$L^1\Pi_f$, $v = 0$	$J = 1$	328 ± 10	115 ± 40	1400 ± 500
	$J = 2$	344 ± 15	129 ± 40	1200 ± 400
	$J = 3$	400 ± 20	185 ± 50	860 ± 230
	$J = 4$	397 ± 30	182 ± 50	870 ± 240
	$J = 5$	365 ± 30	150 ± 50	1100 ± 300
	$J = 6$	359 ± 30	144 ± 50	1100 ± 300
$L^1\Pi_e$, $v = 0$	$J = 1$	690 ± 40	500 ± 60	320 ± 40
$K^1\Sigma^+$, $v = 0$	$J = 0$	3250 ± 300	3000 ± 300	53 ± 5
	$J = 1$	3250 ± 300	3000 ± 300	53 ± 5
	$J = 2$	3100 ± 300	2850 ± 300	56 ± 5
	$J = 3$	3350 ± 300	3100 ± 300	51 ± 5
$W^1\Pi_f$, $v = 0$	$J = 1$	1500 ± 100	1250 ± 120	130 ± 10
	$J = 2$	1510 ± 100	1250 ± 120	130 ± 10
	$J = 3$	1520 ± 150	1250 ± 160	130 ± 15

The instrumental linewidth had to be deconvoluted from the observed widths to deduce the natural linewidth expressed as Γ. The $5p^6$–$6s'$ resonance line of ^{84}Kr appeared to have a width of 250 ± 30 MHz at the lowest laser intensities. This value includes the bandwidth of the XUV source and a small contribution of Doppler broadening in the atomic beam. The observed instrumental profile was close to a Lorentzian. A convolution of two Lorentzian functions with linewidths Γ_1 and Γ_2 produces again a Lorentzian of width $\Gamma = \Gamma_1 + \Gamma_2$. Consequently the instrument function can be deconvoluted from the observed widths by subtracting 250 MHz. However, even small deviations from a Lorentzian will affect the correctness of the deconvolution. Particularly for the observed widths of the Q-branch lines of the L–X (0, 0) band, which lie in the range 325–400 MHz and only marginally exceed the instrumental width, the specific line shape is important. From numerical deconvolution tests of the actual line shapes, we found that subtraction of 215 MHz (corresponding to 85% of the instrument width) yields the most reliable values for the natural linewidths of the narrow CO features. This deconvolution procedure introduces uncertainties in Γ larger than the uncertainties in $\delta\nu_{obs}$ resulting from the fitting procedure. For this reason we quote error margins of 30% on the lifetimes of the $L^1\Pi_f$ state. For the broader lines in the other bands the uncertainties in the values for Γ derive from the fitting procedure. Values of Γ and lifetimes $\tau(\tau = 1/2\pi\Gamma)$ for all the states investigated are given in Table 1 as well. Only lines observed with sufficient signal-to-noise ratios for a linewidth determination were included.

Within the experimental uncertainty the lifetimes of the f component of the $W^1\Pi$ and $L^1\Pi$ states, as well as of the $K^1\Sigma^+$ state are independent of J. Therefore J-averaged values are calculated, resulting in $\tau = 130 \pm 10$ ps for the $W^1\Pi_f$, $v = 0$ state ($J = 1$–3); $\tau = 54 \pm 5$ ps for the $K^1\Sigma^+$, $v = 0$ state ($J = 0$–3); and $\tau = 1.0 \pm 0.3$ ns for the $L^1\Pi_f$, $v = 0$ state ($J = 1$–6). For the $L^1\Pi_f$ state the systematic uncertainty of 30% was included in the error margin of the averaged value.

B. Absolute Frequency Calibration of CO Lines in the Extreme Ultraviolet

In a previous study,[1] transitions of the W–X (0, 0), L–X (0, 0), and K–X (0, 0) bands were calibrated on an absolute frequency scale by comparing and intrapolating the XUV resonances with simultaneously recorded Doppler-broadened I_2-absorption spectra. This Doppler-broadened I_2 standard is insufficiently accurate to fully employ the narrow linewidth of the CO resonance in calibration. The widths of the I_2-absorption lines (1 GHz in the visible) correspond to a 6-GHz width on the XUV scale. A solution is to use hyperfine components of I_2, resolved by Doppler-free saturation spectroscopy. In Fig. 5 a recording of the narrow $Q(1)$ line of the L–X (0, 0) band is shown with simultaneously recorded saturated I_2 absorption and etalon spectra. The etalon markers are used to construct a linearized frequency scale on which the CO resonance line position can be determined with respect to an I_2-marker line. This possibility for absolute calibration in the XUV domain was already demonstrated in a recent study of the transition frequency of the 58-nm resonance line in the He atom[10] and is applied here in a spectroscopic study of a molecule.

In our laboratory no equipment is available for direct absolute frequency measurements at megahertz accuracy. Such instruments at present exist only in national metrology laboratories (e.g., the National Institute of Standards and Technology, Gaithersburg; Bureau National de Métrologie, Paris; and the Physikalische Technische Bundesanstalt, Braunschweig). Relative measurements with respect to a calibrated standard, using a stable etalon, can, however, be performed in many laboratories, and we followed this procedure for absolute cali-

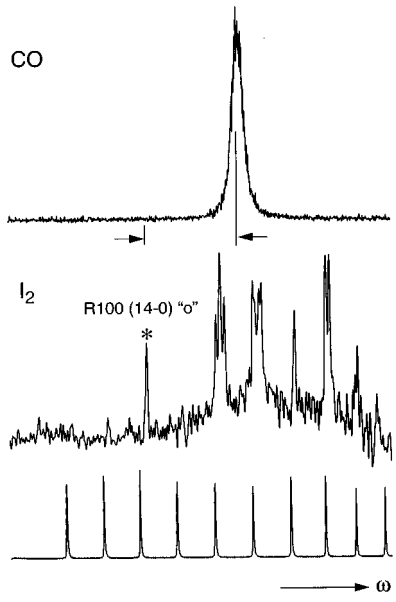

Fig. 5. Spectrum of the $Q(1)$ line of the $L^1\Pi$–$X^1\Sigma^+(0, 0)$ band of CO recorded simultaneously with a Doppler-free I_2 spectrum and an etalon spectrum. This spectrum was recorded from a pure CO beam, without use of the EOM for chirp compensation. The absolute frequency of the $Q(1)$ line is calibrated with respect to the I_2 line marked by an asterisk at 17 211.96456(20) cm^{-1}.

bration of the CO lines. For the yellow wavelength range ~30 saturated I_2 lines are reported in the literature.[7–9] None of these lines was close enough to the fundamental frequency used for excitation of the $L\,^1\Pi$ state. Therefore we used the value of the t component of the $P98\,(14–0)$ line at 17 205.788934 cm^{-1} or 515 816 575.64 MHz as an absolute reference.[14]

In a separate experiment the frequency range from the reference at 17 205 cm^{-1} to the fundamental for the $L\,^1\Pi$ state of CO at 17 213 cm^{-1} was calibrated absolutely. For this purpose a 633-nm He–Ne laser, intracavity locked to an I_2-hyperfine component was used to stabilize the length of an etalon (see Fig. 1). Both the He–Ne laser and the etalon were locked to the same mode during the entire calibration procedure, which lasted many hours. First the FSR of the stabilized etalon was determined by scanning the yellow ring dye laser and counting the number of fringes between the accurately calibrated $P98$ (14–0) t line,[14] the $R99$ (15–1) line at 512 667 622.78 MHz,[9] the $P94$ (15–1) o line at 512 680 508.7 MHz,[7] and the $P80$ (16–2) o line at 510 098 229.4 MHz.[7] This results in a consistent FSR value of 148.9560 (5) MHz.

After a determination of the FSR, the I_2-saturation absorption spectrum in the range 17 205–17 213 cm^{-1} was covered with overlapping scans for an approximate determination of the frequency spacing in terms of the number of frequency markers. Subsequently several I_2 hyperfine components were recorded in slow scans for a highly precise measurement. All recorded data handling was stored in a computer. The frequency scale was linearized by spline fitting the etalon spectra. The positions of the I_2-saturation components [including the $P98$ (14–0) t reference] were determined by computerized interpolation, yielding accurate values for their absolute frequencies. In this way, 14 I_2-hyperfine components were calibrated; since these data may be of value for future spectroscopic research, they are listed in Table 2. For convenience the hyperfine components at the low-energy side of the multiplet are calibrated, in the case of even J, the o components and in the case of odd J, the w components. The uncertainty in the frequencies is determined by the accuracy of the fitting procedure, the accuracy of the reference line (<1 MHz), and the accuracy of the FSR. The I_2-saturation spectra were recorded at room-temperature vapor pressure, without specifically reproducing the conditions under which the original calibrations had taken place. Temperature and pressure effects for such circumstances may give rise to shifts of the order of 1 MHz. Combining all error sources, the final uncertainties in the recorded I_2 transitions are estimated at 4–5 MHz.

The Q-branch lines of the $L–X$ (0, 0) band of CO were measured in simultaneous recordings with I_2-saturation spectra and etalon fringes. From separations between CO lines and I_2 components (see Table 2) absolute frequencies in the XUV domain were determined after multiplication by 6 for the harmonic conversion. Again all spectra were fitted by computer, and scale linearization also was employed. A statistical uncertainty related to the multiple recording of a single strong line is estimated to be 5–20 MHz, depending on the signal-to-noise ratio, and the uncertainty of the XUV-frequency scale, because of the use of the saturated I_2 components, is 30 MHz. Three systematic effects, which may give rise to frequency shifts, were addressed. First a small deviation from exact perpendicular alignment between light and molecular beam may cause a Doppler shift. This phenomenon was investigated by varying the velocity of CO molecules in the molecular beam. The frequencies of the $Q(1)$ line were determined for a pure CO beam (average velocity 660 m/s) and for a beam of CO seeded in Kr (average velocity 380 m/s) in conditions of supersonic expansion. In the latter, the lines were found to be blue shifted by 43 MHz. In extrapolation to zero transversal velocities a Doppler-shift correction of 75 ± 40 MHz is determined. A second important systematic effect results from the phenomenon of frequency chirp, which gives rise to an offset between the seed frequency of the cw ring dye laser and the frequency of the pulsed laser, averaged over the pulse duration. In a series of measurements, for which the chirp was compensated, we found a chirp-induced redshift of 68 ± 50 MHz (on the XUV scale). The method for the generation of nearly chirp-free pulses from a PDA is described elsewhere.[11] Finally, an uncertainty that is due to the ac–Stark effect and is induced by the intense UV-laser light present in the interaction region is estimated to be 50 MHz, since no effects were observed. Measurements on an atomic system[11] yielded clearly observable ac–Stark-induced line shifts. Combining all unrelated sources of error yields an estimate for the uncertainty in the absolute frequency of the Q-branch lines of 90 MHz or 0.003 cm^{-1}. The resulting transition frequencies are listed in Table 3 for the $Q(1)$ to $Q(12)$ lines measured here.

Many of the factors contributing to uncertainty in the absolute frequency of the CO lines are the same throughout the Q branch of the $L–X$ (0, 0) band. For relative measurements of frequency separations between $Q(J)$ and $Q(J + 1)$ lines in terms of etalon fringes, in fact only the statistical error of the fitting procedure remains,

Table 2. I_2 Hyperfine Components Calibrated in the Present Study[a]

Iodine Line	Frequency (MHz)	Frequency (cm^{-1})	I_2 Atlas
$R95$ (16–1) w	515 827 579.5 (40)	17 206.15598 (13)	1425
$R83$ (18–2) o	515 870 592.7 (40)	17 207.59075 (13)	1430
$R94$ (16–1) o	515 889 490.4 (40)	17 208.22111 (13)	1434
$P89$ (16–1) w	515 909 718.2 (40)	17 208.89583 (13)	1438
$R82$ (18–2) o	515 925 934.8 (40)	17 209.43676 (13)	1440
$R93$ (16–1) w	515 950 679.2 (40)	17 210.26215 (13)	1445
$P88$ (16–1) o	515 970 647.8 (40)	17 210.92823 (13)	1448
$R81$ (18–2) w	515 980 528.1 (50)	17 211.25780 (17)	1449
$P126$ (17–1) o	515 991 989.1 (50)	17 211.64010 (17)	1451
$R100$ (14–0) o	516 001 716.4 (60)	17 211.96456 (20)	1453
$P76$ (18–2) o	516 008 245.5 (50)	17 212.18235 (17)	1455
$R92$ (16–1) o	516 011 235.3 (50)	17 212.28208 (17)	1457
$P87$ (16–1) w	516 030 852.3 (50)	17 212.93643 (17)	1459
$R80$ (18–2) o	516 034 479.8 (50)	17 213.05743 (17)	1460

[a] Values are a result of relative frequency measurements with respect to the $P98$ (14–0) t component, determined by Sansonetti at 515 816 575.64 MHz.[14] The numbers in the last column refer to the identification of Doppler-broadened lines in the I_2 atlas.[6]

which is of the order of 8 MHz for the separation of strong lines and up to 20 MHz for the weaker lines. These highly accurate frequency separations between Q lines are listed in Table 4.

All values, absolute and relative frequencies, are included in a least-squares fit together with the less accurate values, up to $Q(22)$, from the absolute frequency measurements from the previous investigation.[1] In the fit the energy levels of the $X^1\Sigma^+$, $v = 0$ ground state were calculated with recent accurate molecular constants of Varberg and Evenson.[15] First the resulting constants for the $L^1\Pi_f$, $v = 0$ state in a simple rotor model fitting $E(J) = v_0 + BJ(J+1) - DJ^2(J+1)^2$ are given in Table 5. This is referred to as model (a) in Tables 3–5. Since the absolute accuracy of the previous measurements[1] was limited, the data for $Q(13)$–$Q(22)$ were allowed to shift over a constant value in the least-squares routine. An optimum is found for a shift of 0.09 cm^{-1}, which is within the stated uncertainty.[1] The lines $Q(1)$–$Q(6)$ gradually shift upward, while Q lines for $J > 7$ shift downward in frequency. From these deviations it clearly follows that an anticrossing occurs near the missing $J = 7$ level.

Subsequently a deperturbation analysis was performed in which a bound state is assumed with a certain v_0 and rotational constant B, interacting homogeneously with the $L^1\Pi_f$, $v = 0$ state with a constant interaction matrix element W_{int}. Such a procedure, referred to as model (b), was described by Eikema *et al.*[16] Again the data pertaining to the absolute frequencies (Table 3) and frequency separations (Table 4) were included in a least-squares fit, resulting in the molecular parameters given in the last column of Table 5. In this model the absolute data are found to fit better than 0.001 cm^{-1}, while the frequency separations are found to fit better than 10 MHz. The observed frequency separation between $Q(11)$ and $Q(10)$, which was left out of the fit, is 75 MHz smaller than calculated. At the present level of accuracy this is a strong indication for a second local perturbation between $J = 10$ and $J = 11$ levels in the $L^1\Pi_f$, $v = 0$ manifold.

Table 3. Observed and Calculated Line Positions (in cm^{-1}) of the Q Lines of the $(4p\pi)$ $L^1\Pi$–$X^1\Sigma^+$ (0,0) Band of $^{12}C^{16}O$ at $\lambda = 96.83$ nm[a]

		Observed–Calculated	
J	Transition Frequency	(a)	(b)
1	103 271.8641 ± 0.0030	0.0026	0.0001
2	103 272.0134 ± 0.0030	0.0024	0.0001
3	103 272.2369 ± 0.0030	0.0017	−0.0002
4	103 272.5363 ± 0.0030	0.0024	0.0005
5	103 272.9097 ± 0.0030	0.0025	−0.0001
6	103 273.3620 ± 0.0030	0.0072	−0.0003
7	–	–	–
8	103 274.4611 ± 0.0040	−0.0112	0.0010
9	103 275.1337 ± 0.0040	−0.0082	0.0011
10	103 275.8780 ± 0.0050	−0.0069	0.0009
11	103 276.6913 ± 0.0050	−0.0100	−0.0035
12	103 277.5852 ± 0.0050	−0.0053	−0.0008
13	103 278.57 ± 0.10	−0.11	−0.08
14	103 279.57 ± 0.10	−0.15	−0.12
15	103 280.77 ± 0.10	−0.05	−0.03
16	103 281.96 ± 0.10	−0.04	−0.02
17	103 283.27 ± 0.10	0.02	0.03
18	103 284.62 ± 0.10	0.05	0.05
19	103 286.03 ± 0.10	0.07	0.06
20	103 287.50 ± 0.10	0.08	0.05
22	103 290.66 ± 0.10	0.12	0.05

[a] Values for levels $J > 12$ are taken from Ref. 1. Values in cm^{-1}. (a) and (b) refer to models for analyzing the data (see text).

Table 4. Frequency Separations between Q Lines of the L–X (0, 0) Band of CO and Deviations from a Least-Squares Fit[a]

		Observed–Calculated	
Frequency Separation	Observed	(a)	(b)
$Q(2)$–$Q(1)$	4 474 ± 8	−8	1
$Q(3)$–$Q(2)$	6 709 ± 8	−11	−3
$Q(4)$–$Q(3)$	8 960 ± 10	3	6
$Q(5)$–$Q(4)$	11 214 ± 10	24	2
$Q(6)$–$Q(5)$	13 566 ± 10	147	−1
$Q(9)$–$Q(8)$	20 162 ± 15	89	1
$Q(10)$–$Q(9)$	22 313 ± 15	36	−5
$Q(11)$–$Q(10)$	24 439 ± 15[b]	−33	−75
$Q(12)$–$Q(11)$	26 719 ± 15	59	1

[a] All values in megahertz.
[b] Not included in the fit.

Table 5. Molecular Constants for f Components of the $L^1\Pi$, $v = 0$ State, Resulting from a Least-Squares Fit Including All Data from Tables 3 and 4[a]

	Model	
Constant	(a)	(b)
ν_0	103 271.787 (4)	103 271.7870 (5)
B	1.9599 (1)	1.95978 (2)
D	7.3 (5) × 10^{-6}	6.59 (5) × 10^{-6}
W_{int}	–	0.22 (1)
ν_0 (pert)	–	103 266.92 (3)
B (pert)	–	2.051 (1)

[a] Values are given in inverse centimeters.

4. DISCUSSION AND CONCLUSION

It has been demonstrated that a narrow-band XUV-laser source can be employed to determine the lifetimes of excited states of molecules. In the range up to 300 ps, accurate values can be determined straightforwardly, while in the range up to 1 ns, lifetime values critically depend on the deconvolution of the instrument width, giving rise to relatively large uncertainties. It has already been demonstrated that, in such an instrument, lifetimes as short as 3 ps can be measured as well,[1] so that now a dynamic range of two orders of magnitude for lifetime measurements is covered. This dynamic range is attractive for the determination of, e.g., rotational-state-dependent predissociation rates for the excited states of CO. At 1 ns

the limit of radiative decay is met for most excited states; this limit can now be reached by narrow-band XUV-laser excitation.

Letzelter *et al.*[17] have established that photodissociation of CO occurs mainly through absorption to bound states, which are coupled to dissociative continua. A subsequent comprehensive study by Eidelsberg and Rostas[18] yielded values for the rates of predissociation, which were accurate to a factor of three. Laser spectroscopic techniques, involving line-broadening measurements, were developed that improved accuracies to the 10% level.[1,2,4,19] A compilation of predissociation rates and lifetimes, including rotational-state and isotopic dependencies, was recently published.[20] Since the studies of Letzelter *et al.*,[17] all excited states of CO in the energy range above 100 000 cm^{-1} are considered to be predissociative with a predissociation yield of $\eta_{dis} > 99\%$. These measurements were, however, performed in low resolution, and no distinction could be made between, e.g., *e*/*f* components of the same $^1\Pi$ state. It was found that in several states the predissociation rate depends strongly on the rotational quantum number and the *e*/*f* parity.[1,2] From these dependencies it was concluded that predissociation in the $K^1\Sigma^+$ state and in the Π_e components of the $W^1\Pi$ and $L^1\Pi$ states is caused by strong coupling with the repulsive part of the $D'^1\Sigma^+$ state, which was observed by Wolk and Rich[21] in its lower energy region. In recent close-coupling calculations it was shown that this $D'^1\Sigma^+$ state also causes the predissociation of the $B^1\Sigma^+$ state.[22] The weaker predissociation of the Π_f components of the $W^1\Pi$ and $L^1\Pi$ states cannot be attributed to a state of $^1\Sigma^+$ symmetry, and the perturber state has yet to be identified.

Drabbels *et al.*[2] performed a double-resonance experiment in which the same states were probed by a narrow-band laser (135 MHz) in the visible. For the $K^1\Sigma^+$, $v = 0$ state and the $W^1\Pi_f$, $v = 0$ state they found linewidths of 3540 ± 200 MHz and 1530 ± 120 MHz, respectively, within error limits that are in agreement with present findings. For the $L^1\Pi_f$, $v = 0$ state they observed the $J = 2-3$ levels and derived a lifetime of 0.55 ns. A lifetime of 0.55 ns corresponds to a natural width of 290 MHz, which is very near the narrowest lines observed in the present study (330 MHz). In view of the effects of the instrument in our experiment this difference definitely must be larger. In the experiment of Drabbels *et al.*[2] the bandwidth profile of their laser source was assumed to be Gaussian in their deconvolution procedure. Small Lorentzian-like contributions in the wings, which may have been overlooked, could strongly affect the outcome of the deconvolution followed in Ref. 2. This might explain the discrepancy. We note that experimental artifacts, e.g., collisional effects, usually tend to broaden rather than narrow spectral lines.

For the $W^1\Pi$ state, the lowest-energy Rydberg state converging to the electronically excited ion core $A^2\Pi$, *ab initio* calculations have been performed by Kirby and coworkers.[23,24] A total radiative decay rate of 25.2 × 10^7 s^{-1} was derived, corresponding to a radiative lifetime of 4 ns. From the presently obtained lifetime of 130 ps it follows that even the Π_f component of the $W^1\Pi$, $v = 0$ state is predissociated for 96.6%. Since the potential minimum of the $W^1\Pi$ state is shifted with respect to the ground state, the 3.3% radiative decay will populate vibrationally excited states of the electronic ground configuration. Kirby *et al.* also calculated a radiative decay rate of 1.3×10^7 s^{-1} to the long-lived $I^1\Sigma^-$ and $D^1\Delta$ states,[24] because of their metastability these states may play an important role in chemistry. We derive an excitation probability of these states through excitation of the $W^1\Pi_f$, $v = 0$ state of 0.15%.

For the lifetime of the $4p\pi L^1\Pi$ state no *ab initio* calculations are available. Our present value of 1.0 ± 0.3 ns is as might be expected for a purely radiative decay of a highly excited singlet state. If indeed the *f* components of the $L^1\Pi$ state do not predissociate or do so by only a small percentage, this may have some important consequences for astrochemistry. For the states $L^1\Pi_f$, with $J \neq 7$, we find a rotationally independent lifetime. At the same time the missing $Q(7)$ line in the two-photon ionization process is clear proof of the rotationally dependent lifetime. The behavior of an accidental predissociation was also observed by Sekine *et al.*[13]

A phenomenon of a global predissociation throughout the rotational manifold can be caused by homogeneous coupling to a state of $^1\Pi$ symmetry, which is repulsive in this energy region. Such a state was recently identified in *ab initio* calculations of CO.[25] An accidental predissociation must be caused by another unidentified bound state that nearly coincides in energy with the $L^1\Pi$ state at $J = 7$. From the matrix diagonalization in the deperturbation analysis, based on the level shifts, it follows that the $J_f = 7$ level has an admixture of 33% perturber state, while all other rotational levels have less than 2% perturber-state character. This explains why broadening effects are not observed for $J \neq 7$ states.

The $L^1\Pi$ state is known to be part of a $4p$–Rydberg complex, while it also homogeneously interacts with a valence state of $^1\Pi$ character.[26] Interaction with the $L'^1\Pi$ state, which is off by 60 cm^{-1} for all J levels, will not cause an anticrossing, while the $4p\sigma^1\Sigma^+$ state only affects *e*-symmetry levels. From the deperturbation analysis it follows that the perturber state has a rotational constant of 2.05 cm^{-1} and must therefore be a Rydberg state. Since the perturber interacts with the *f* symmetry levels, it is of either Σ^- or Π character. A similar example of an accidental predissociation was recently analyzed for the $E^1\Pi$, $v = 1, J = 7$ level of CO,[19] which was attributed to an interaction with the $k^3\Pi$ triplet state. That the $L^1\Pi_f$ state is also slightly perturbed between $J = 10$ and $J = 11$ makes this example particularly similar to that of the $E^1\Pi$ state, so the perturber state is possibly a $^3\Pi$ state as well.

Transition frequencies of molecular absorption lines in the extreme ultraviolet domain have been determined within 0.003 cm^{-1}. We note that energies of highly excited states in atomic hydrogen[27] and molecular hydrogen[28] have been determined with higher accuracy, but this was done in two-photon experiments employing UV lasers. We also refer to the accurate calibration of the He-resonance line at 58 nm by our group.[11] The measured transition frequencies in this work may be used in the future as a wavelength standard near 96 nm. In principle the method presented here can be extended to

many other molecules and to a much wider wavelength range. However, the lack of accurately known (1-MHz level) reference lines still limits its applicability. For this reason the observed lines in the $K-X$ (0, 0) and $W-X$ (0, 0) bands could not be calibrated against I_2 saturation components, because nearby calibrated reference lines are not available. If reference lines are separated by more than 10 cm^{-1} (at the fundamental frequency) from the XUV-resonance lines, the method of absolute calibration by scanning the fringes of a stabilized etalon becomes unpractical and less precise. Future progress in XUV-precision spectroscopy depends on the availability of a large number of accurately calibrated reference lines in the visible domain.

ACKNOWLEDGMENTS

The authors express their sincere thanks to C. Sansonetti, National Institute of Standards and Technology, Gaithersburg, Maryland, for making available the accurate calibration of the $P98(14-0)t$ line of iodine, which was used as an absolute reference in this study. They also thank R. van Dierendonck for discussions on the I_2-calibration procedures. This work was financially supported by the Netherlands Foundation for Fundamental Research.

REFERENCES

1. K. S. E. Eikema, W. Hogervorst, and W. Ubachs, "Predissociation rates in carbon monoxide: dependence on rotational state, parity and isotope," Chem. Phys. **181**, 217 (1994).
2. M. Drabbels, J. Heinze, J. J. ter Meulen, and W. L. Meerts, "High resolution double-resonance spectroscopy on Rydberg states of CO," J. Chem. Phys. **99**, 5701 (1993).
3. T. Trickl, M. J. J. Vrakking, E. Cromwell, Y. T. Lee, and A. Kung, "Ultra-high resolution (1 + 1) photoionization spectroscopy of Kr I: hyperfine structures, isotope shifts, and lifetimes for the $n = 5$, 6, 7 $4p^5ns$ Rydberg levels," Phys. Rev. A **39**, 2948 (1989).
4. P. F. Levelt, W. Ubachs, and W. Hogervorst, "Extreme ultraviolet laser spectroscopy on CO in the 91–100 nm range," J. Chem. Phys. **97**, 7160 (1992).
5. K. S. E. Eikema, W. Ubachs, and W. Hogervorst, "Isotope shift in the neon ground state by extreme ultraviolet laser spectroscopy at 74 nm." Phys. Rev. A **49**, 803 (1994).
6. S. Gerstenkorn and P. Luc, *Atlas du Spectre d'Absorption de la Molecule de l'Iode Entre 14800–20000 cm*$^{-1}$ (CNRS, Paris, 1978).
7. L. Hlousek and W. H. Fairbank, "High-accuracy wavenumber measurements in molecular iodine," Opt. Lett. **8**, 322 (1983).
8. D. Shiner, J. M. Gilligan, B. M. Cook, and W. Lichten, "H_2, D_2, and HD ionization potentials by accurate calibration of several iodine lines," Phys. Rev. A **47**, 4042 (1993).
9. R. Grieser, G. Bönsch, S. Dickopf, G. Huber, R. Klein, P. Merz, A. Nicolaus, and H. Schnatz, "Precision measurement of two iodine lines at 585 nm and 549 nm," Z. Phys. A **348**, 147 (1994).
10. K. S. E. Eikema, W. Ubachs, W. Vassen, and W. Hogervorst, "Precision measurement in helium at 58 nm: the ground state Lamb shift and the 1^1S-2^1P transition isotope shift," Phys. Rev. Lett. **76**, 1216 (1996).
11. K. S. E. Eikema, W. Ubachs, W. Vassen, and W. Hogervorst, "Lamb shift measurements in the 1^1S ground state of helium," Phys. Rev. A **55**, 1866 (1997).
12. E. Cromwell, T. Trickl, Y. T. Lee, and A. Kung, "Ultranarrow bandwidth VUV–XUV laser system," Rev. Sci. Instrum. **60**, 2888 (1989).
13. S. Sekine, T. Masaki, Y. Adachi, and C. Hirose, "Optogalvanic spectrum of CO. II. The rotational structure of the $L^1\Pi$ state," J. Chem. Phys. **89**, 3951 (1988).
14. C. Sansonetti, "Precise measurements of hyperfine components in the spectrum of molecular iodine," J. Opt. Soc. Am. B **14**, 1913 (1997).
15. Th. D. Varberg and K. M. Evenson, "Accurate far-infrared rotational frequencies of carbon monoxide," Astrophys. J. **385**, 763 (1992).
16. K. S. E. Eikema, W. Hogervorst, and W. Ubachs, "On the determination of a heterogeneous vs a homogeneous perturbation in the spectrum of a diatomic molecule: the $K^1\Sigma^+$, $v = 0$ state of $^{13}C^{18}O$," J. Mol. Spectrosc. **163**, 19 (1994).
17. C. Letzelter, M. Eidelsberg, F. Rostas, J. Breton, and B. Thieblemont, "Photoabsorption and photodissociation cross sections of CO between 88.5 and 115 nm," Chem. Phys. **114**, 273 (1990).
18. M. Eidelsberg and F. Rostas, "Spectroscopic, absorption and photodissociation data for CO and isotopic species between 91 and 115 nm," Astron. Astrophys. **235**, 472 (1990).
19. P. C. Cacciani, W. Hogervorst, and W. Ubachs, "Accidental predissociation phenomena in the $E^1\Pi$, $v = 0$ and $v = 1$ states of $^{12}C^{16}O$ and $^{13}C^{16}O$," J. Chem. Phys. **102**, 8308 (1995).
20. W. Ubachs, K. S. E. Eikema, P. F. Levelt, W. Hogervorst, M. Drabbels, W. L. Meerts, and J. J. ter Meulen, "Accurate determination of predissociation rates and transition frequencies of carbon monoxide," Astrophys. J. Lett. **427**, L55 (1994).
21. G. L. Wolk and J. W. Rich, "Observation of a new electronic state of carbon monoxide using LIF on highly vibrationally excited CO($X^1\Sigma^+$)," J. Chem. Phys. **79**, 12 (1983).
22. W. Tchang-Brillet, P. S. Julienne, J. M. Robbe, C. Letzelter, and F. Rostas, "A model of the $B^1\Sigma^+-D'^1\Sigma^+$ Rydberg-valence predissociating interaction in the CO molecule," J. Chem. Phys. **96**, 6735 (1992).
23. D. L. Cooper and K. Kirby, "Theoretical study of the $(3s\sigma)^1\Pi$ Rydberg state of CO," Chem. Phys. Lett. **152**, 393 (1988).
24. K. Kirby, M. E. Rosenkrantz, and D. L. Cooper, "Population of long-lived vibrational levels of CO: $I^1\Sigma^-$ and $D^1\Delta$," Phys. Rev. Lett. **68**, 3865 (1992).
25. M. Hiyama and H. Nakamura, "Superexcited states of CO near the first ionization threshold," Chem. Phys. Lett. **248**, 316 (1996).
26. F. Rostas, F. Launay, M. Eidelsberg, M. Benharrous, C. Blaes, and K. P. Huber, "Extreme UV absorption spectroscopy of CO isotopomers in pulsed supersonic free jet expansions," Can. J. Phys. **72**, 913 (1994).
27. M. Weitz, A. Huber, F. Schmidt-Kaler, D. Leibfried, W. Vassen, C. Zimmerman, K. Pachucki, T. W. Hänsch, L. Julien, and F. Biraben, "Precision measurement of the $1S$ ground-state Lamb shift in atomic hydrogen and deuterium by frequency comparison," Phys. Rev. A **52**, 2664 (1995).
28. E. E. Eyler, J. Gilligan, E. McCormack, A. Nussenzweig, and E. Pollack, "Precise two-photon spectroscopy of $EF-X$ intervals in H_2," Phys. Rev. A **36**, 3486 (1987).